

Development of a Steam Distribution Network Simulator for Enhanced Oil Recovery Systems

***Tatsuro Yashiki¹, Yukinori Katagiri¹, Yoshikazu Ishii¹,
Shunichi Kuba², Takayuki Mitadera³, and Tomohiko Yoshida²**

¹Hitachi, Ltd., Hitachi Research Laboratory, 7-2-1, Omika-cho, Hitachi-shi, Ibaraki, Japan

²Hitachi, Ltd., Hitachi Power Systems Company, 3-1-1 Saiwai-cho, Hitachi-shi, Ibaraki, Japan

³Hitachi Power Solutions Co., Ltd., 3-1-1, Saiwai-cho, Hitachi-shi, Ibaraki, Japan

*Corresponding author: tatsuro.yashiki.zn@hitachi.com

Abstract

Enhanced oil recovery (EOR) by injecting steam into oil wells is widely used to make the oil less viscous, thereby improving its mobility and recovery. Steam is generated by steam generators and supplied to oil wells through a steam distribution network. In order to optimize the effects of EOR, it is necessary to predict steam properties in the distribution network with high accuracy. In this paper, a newly developed steam distribution network simulator for EOR systems is introduced. The features of the simulator are providing: (1) a highly accurate prediction of steam properties including phase change (steam to drain) in a complex steam distribution network by adopting a pipe flow model using the finite volume method and the Newton-Raphson method and a steam distribution network flow model according to graph theory and (2) a dedicated interface for operators to build the steam distribution network model easily by referring to a topographic map. The simulation results show that the developed simulator is useful to evaluate and modify an existing steam distribution network and to design a new one.

Keywords: Steam Distribution Network, Simulator, Two-phase Flow, EOR.

Introduction

Enhanced oil recovery (EOR) by injecting steam into oil wells has been the most widely used recovery method for heavy and extra-heavy oil production in sandstone reservoirs. For the steam injection, several steam generators are located throughout the oil field to produce the steam that is fed into a distribution network. As the distribution network becomes more complex and larger, the steam flow becomes more complicated and the steam properties along the pipes vary greatly. Additionally the heat loss from the pipe to the surrounding air makes the steam condense into a drain and these condensations also complicate the steam flow. Thus, the effective operation of the EOR systems requires an understanding of the steam flow in the distribution network that may be done using numerical simulation.

The requirements for the steam distribution network simulation of EOR systems are: (1) providing highly accurate prediction of steam properties including phase change (steam to drain); (2) having applicability to complex and large distribution networks with multiple loops, steam generators and oil wells; and (3) realizing easy building of a distribution network model for the simulation. Many studies on the fluid and heat flow in a distribution network have been reported. However most of the mathematical models or computer programs that were developed in these studies do not satisfy the above-mentioned requirements simultaneously. Majumdar et al. (1997) developed a computer program for analyzing steady compressible flow with phase change and heat transfer in a complex distribution network. This program involves complicated procedures for operators to build a distribution network model with long distance pipes, since the operators must divide each of the pipes into many partial pipes to predict steam properties with high accuracy. This paper describes a

newly developed steam distribution network simulator for EOR systems. The simulation results are a highly accurate prediction of steam properties including the phase change. The results also show that the developed simulator is useful to evaluate and modify an existing steam distribution network and to design a new steam distribution network.

Mathematical model of pipe flow

The following three sections describe the mathematical model and the user interface developed to satisfy the above-mentioned requirements for the steam distribution network simulation of EOR.

Governing equations

In this paper, the pipe flow is assumed to be one-dimensional steady compressible flow with phase change and heat transfer. Additionally the pipe geometry is assumed to be straight with a constant diameter and surrounded by thermal insulation. The governing equations for the pipe flow are the mass conservation, the momentum conservation and the energy conservation equations which are given by

$$\partial \dot{m} / \partial z = 0 \quad (1)$$

$$\partial \left\{ (v \cdot \dot{m}^2) / A \right\} / \partial z + \partial (A \cdot p) / \partial z - A \cdot F_w = 0 \quad (2)$$

$$\partial (\dot{m} \cdot h) / \partial z - P \cdot q_w = 0 \quad (3)$$

where F_w denotes wall friction force and q_w wall heat flux that flows from the pipe to the surrounding air. For the two-phase flow, the slip flow model (JSME, 2006) is chosen. In the slip flow model, the specific volume v in Eq. (2) and the specific enthalpy h in Eq. (3) are given by

$$v = \left\{ (1-x)^2 / (1-\alpha) \right\} v_L + (x^2 / \alpha) v_G \quad (4)$$

$$h = (1-x)h_L + xh_G \quad (5)$$

where the void fraction α is defined using Thom's void fraction correlation (Thom, 1964). To deal with one-phase flow and two-phase flow, the equations for calculating F_w and q_w are switched depending on the phase status of the pipe flow. Details of the equations appear in Appendix A. The independent variables in Eqs. (1), (2) and (3) are mass flow rate, pressure and specific enthalpy. Other thermodynamic properties of steam and water are calculated using the equation of IF97 (IAPWS, 1997)

Discretization of governing equations according to the finite volume method

In order to predict the steam properties with high accuracy, Eqs. (1), (2) and (3) are discretized according to the finite volume method, where the number of control volumes is set to be high enough to resolve the spatial distribution of the properties. The proposed method uses the staggered grid approach (Patankar, 1980) in order to preventing pressure oscillations. In this approach, the mass and energy conservation equations are solved on a control volume grid and the momentum conservation equation is solved on a staggered grid as shown in Fig. 1. The mass flow rate is defined at the staggered grid center and all of the thermodynamic properties are defined at the control volume grid center.

Integrating Eqs. (1) and (3) over the control volume grid gives

$$\dot{m}_{i-1/2} - \dot{m}_{i+1/2} = 0 \quad (6)$$

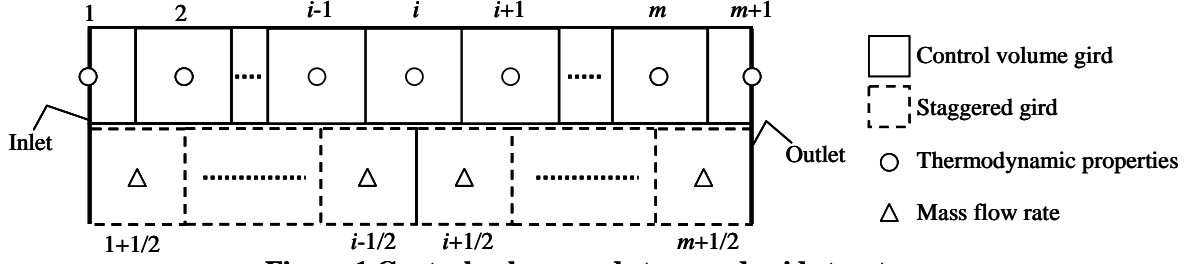


Figure 1 Control volume and staggered grid structure

$$\dot{m}_{i-1/2} \hat{h}_{i-1/2} - \dot{m}_{i+1/2} \hat{h}_{i+1/2} - P_i \Delta z \cdot q_{w,i} = 0 \quad (7)$$

where $\hat{h}_{i-1/2}$ is defined at the control volume grid face. The first order upwind scheme is used to obtain the value of $\hat{h}_{i-1/2}$, thus

$$\dot{m}_{i-1/2} \hat{h}_{i-1/2} = \left\{ (\dot{m}_{i-1/2} + |\dot{m}_{i-1/2}|) / 2 \right\} h_{i-1} + \left\{ (\dot{m}_{i-1/2} - |\dot{m}_{i-1/2}|) / 2 \right\} h_i \quad (8)$$

The value of $\hat{h}_{i+1/2}$ can be obtained in the same way as $\hat{h}_{i-1/2}$. Integrating Eq. (2) over a staggered grid gives

$$v_i (\dot{m}_{i+1/2} / A)^2 - v_{i+1} (\dot{m}_{i+1/2} / A)^2 + p_i - p_{i+1} - \Delta z \cdot K_{i+1/2} \left(|\dot{m}_{i+1/2}| + \dot{m}_\varepsilon \right) \dot{m}_{i+1/2} = 0 \quad (9)$$

Computational scheme using the Newton-Raphson method

The discretized equations (Eqs. (6), (7) and (9)) are non-linear and require iterative calculation. The proposed method applies the Newton-Raphson method (NRM) (Shamir and Howard, 1968), where pressure is corrected so that it satisfies the mass conservation equation (Eq. (6)). The pressure correction equation is given by

$$-\beta_{i-1/2} dp_{i-1} + (\beta_{i-1/2} + \beta_{i+1/2}) dp_i - \beta_{i+1/2} dp_{i+1} = \dot{m}_{i+1/2}^{n-1} - \dot{m}_{i-1/2}^{n-1} \quad (10)$$

$$\beta_{i+1/2} \equiv 1 / \left[2(v_{i+1}^{n-1} - v_i^{n-1}) \dot{m}_{i+1/2}^{n-1} / A^2 + 2K_{i+1/2}^{n-1} \left(|\dot{m}_{i+1/2}^{n-1}| + \dot{m}_\varepsilon \right) \right] \quad (11)$$

where the superscript $n-1$ denotes the previous iteration number. Eq. (10) forms a set of linear equations in terms of dp_i . Once solved, the current iteration pressure p_i^n is updated by

$$p_i^n = p_i^{n-1} + dp_i \quad (12)$$

The current iteration mass flow rate $\dot{m}_{i+1/2}^n$ and specific enthalpy h_i^n are calculated by substituting p_i^n into Eqs. (7) and (9). The calculation process of p_i^n , $\dot{m}_{i+1/2}^n$ and h_i^n is repeated until convergence.

Mathematical model of the steam distribution network flow

Representation of the steam distribution network according to graph theory

According to graph theory, an arbitrary steam distribution network can be represented as a directed linear graph. The network consists of a number of oriented lines connected to nodes as shown in Fig. 2. Lines contain pipes and nodes contain branches, steam sources (steam generators) and steam sinks (oil wells). Lines are connected to one another by nodes and each line is associated with an upstream and a downstream node. The topology of a directed linear graph of N_l lines and N_n nodes can be described by a $N_l \times N_n$ node incidence matrix \mathbf{B} with the typical element:

$$b_{jk} = \begin{cases} +1, & \text{if line } j \text{ is directed away from node } k \\ -1, & \text{if line } j \text{ is directed toward node } k \\ 0, & \text{if line } j \text{ is not connected to node } k \end{cases} \quad (13)$$

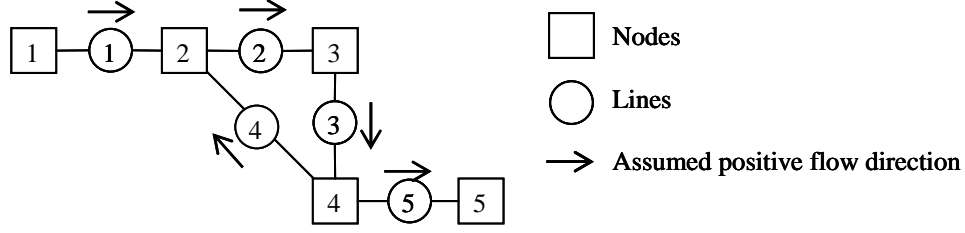


Figure 2 Representation of a network

The node incidence matrix \mathbf{B} for the network shown in Fig. 2 is as follows:

$$\mathbf{B} = \begin{bmatrix} 1 & -1 & 0 & 0 & 0 \\ 0 & 1 & -1 & 0 & 0 \\ 0 & 0 & 1 & -1 & 0 \\ 0 & -1 & 0 & 1 & 0 \\ 0 & 0 & 0 & 1 & -1 \end{bmatrix} \quad (14)$$

Computational scheme

The governing equations for the steam distribution network flow are the mass and the energy conservation equations at nodes and the momentum conservation equation at lines. The proposed method uses the NRM to solve the network flow. In the same way as the pipe flow calculation, the pressure at nodes is calculated by the following pressure correction equation:

$$\mathbf{B} \cdot \begin{bmatrix} y_1 & & 0 \\ & \ddots & \\ 0 & & y_{N_n} \end{bmatrix} \cdot \mathbf{B}^T \cdot \begin{bmatrix} dp_{node,1} \\ \vdots \\ dp_{node,N_n} \end{bmatrix} = \mathbf{B}^T \cdot \begin{bmatrix} \dot{m}_{line,1}^{n-1} \\ \vdots \\ \dot{m}_{line,N_n}^{n-1} \end{bmatrix} \quad (15)$$

$$y_j \equiv \sum_{i=1}^{m_j} \beta_{j,i+1/2} \quad (16)$$

Once $dp_{node,j}$ is solved, the current iteration pressure at nodes $p_{node,j}^n$ is updated by

$$p_{node,k}^n = p_{node,k}^{n-1} + dp_{node,k} \quad (17)$$

Current iteration mass flow rate at lines $\dot{m}_{line,j}^n$ can be computed from the above-mentioned pipe flow model and current iteration specific enthalpy at nodes $h_{node,j}^n$ can be computed from the energy conservation. The calculation process of $p_{node,k}^n$, $\dot{m}_{line,j}^n$ and $h_{node,k}^n$ is repeated until convergence.

User interface of the simulator

The simulator provides a dedicated user interface (Fig. 3) for operators to build the distribution network model easily and to visualize the simulation results. The simulator first takes in a topographic map where the actual distance is associated. Then the operators can build the distribution network model by referring to the map. The pipe length can be calculated automatically using the actual distance associated with the map and the other pipe specifications such as diameter, thickness etc. are defined by the operator inputs. At the beginning of the simulation, each of the pipes is automatically divided into control volumes whose number is set to be high enough to resolve the spatial distribution of the steam properties. In this paper, the pipe is divided into control volumes of 10 meters in length. On the completion of the simulation, the results can be visualized

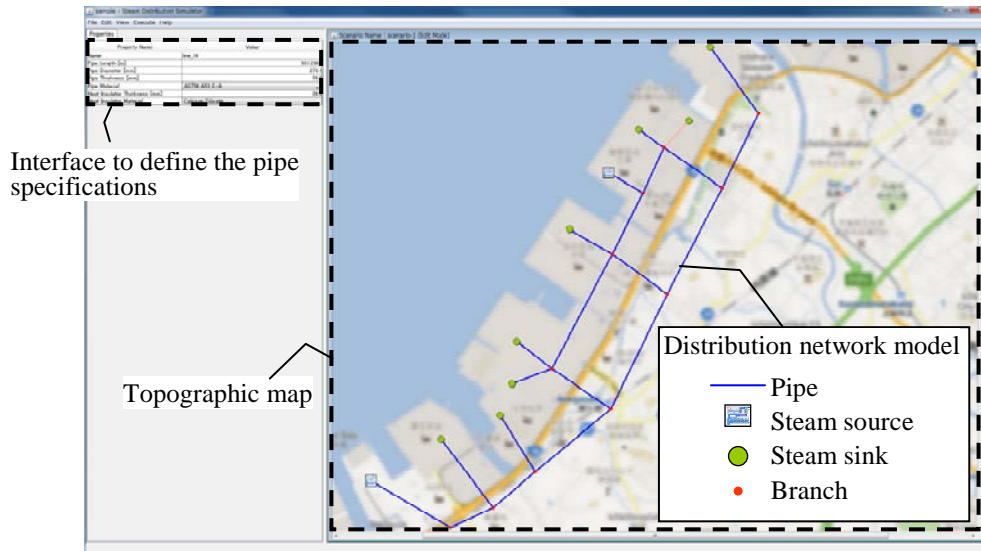


Figure 3 User interface of the developed simulator

as a numeric form or a graphical form. In the provided user interface, the operators can build the distribution network model and calculate the network flow without special knowledge of numerical simulation.

Results and discussion

An example steam distribution network flow was calculated to demonstrate the functionality of the developed simulator. Fig.4 shows the layout of the network that included two loops, two steam sources (nodes 1 and 2) and four steam sinks (nodes 3, 4, 5 and 6). The boundary conditions of the steam sources and steam sinks are given in Fig. 4 and the pipes data are given in Table 1. The pipe thickness and the thermal insulation thickness of all the pipes was 0.03 m. Node 1 supplied superheated steam and node 2 supplied saturated steam.

The results for the example network are shown in Table 2. Because the flow direction for line 13 was left-to-right (from node 6 to node 12), node 1 supplied the steam to nodes 3, 4, 5 and 6, while node 2 supplied the steam to nodes 5 and 6. The steam flowing into nodes 3 and 4 was superheated steam. In contrast, the steam flowing into nodes 5 and 6 was partially condensed into the drain, since the distance from node 1 to node 5 or 6 was far and the heat loss of the steam supplied by node 1 was large. Fig. 5 shows the spatial distribution along lines 17 and 18 flow for five steam properties: pressure, temperature, quality, flow resistance coefficient, and heat transfer coefficient between steam and pipe. The phase status of the pipe flow changed from one-phase flow to two-phase flow at the pipe length of 1230 m. The flow resistance coefficient and heat transfer coefficient were constant over the one-phase region, while they increased throughout the two-phase region due to the steam condensation. Because the developed simulator divides each of the pipes into control volumes automatically and switches the equations of wall friction force and wall heat flux depending on phase status of the pipe flow, it can predict steam properties including phase change with high accuracy.

In order to estimate the effect from degradation of heat insulation, the thermal insulation thickness of lines 17 and 18 was changed from 0.03 m to 0.005 m. The results around lines 17 and 18 for this condition are compared in Table 3 with the original condition (*Italic font*). Because heat loss of lines 17 and 18 increased and large quantities of the steam were condensed, the quality at nodes 6 and 15 decreased. In order to increase the quality at nodes 6 and 15, a mobile steam source that supplied saturated steam was connected to node 15. The steam pressure and temperature supplied

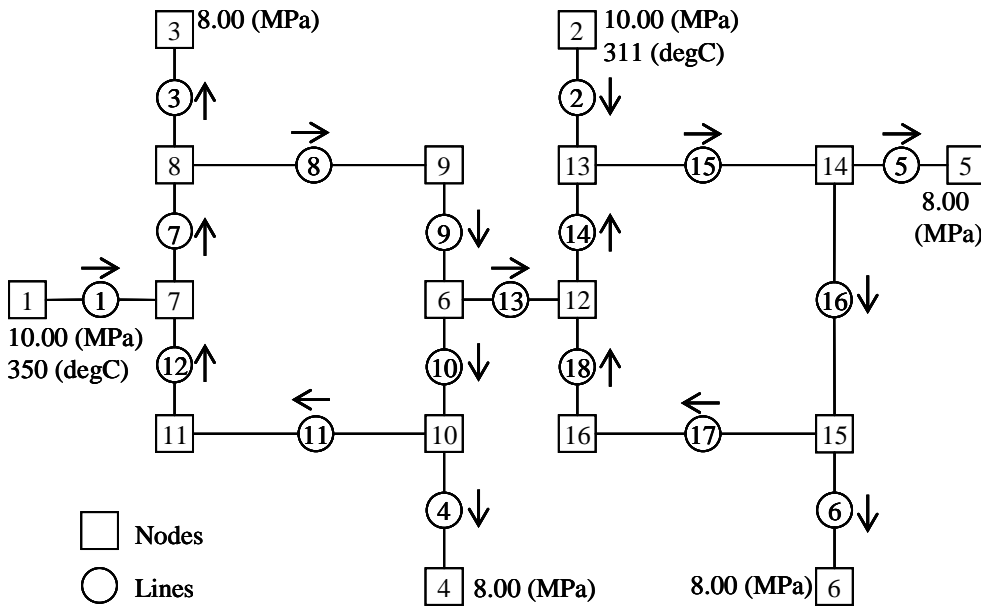


Table 1 Pipes data

Line number	Length (m)	Diameter (m)
1	500	0.2731
2	1000	0.1682
3	500	
4	1000	
5	500	
6	500	
7	750	0.2731
8	2000	
9	750	
10	750	
11	2000	
12	750	
13	1000	
14	750	
15	2000	
16	1500	
17	2000	
18	750	

Figure 4 Layout of the example steam distribution network

Table 2 Results for the example network

Line number	Mass flow rate (kg/s)	Node number	Pressure (MPa)	Temperature (°C)	Quality (-)
1	31.92	1	10.00	350	1.00
2	5.61	2	10.00	311	1.00
3	11.74	3	8.00	325	1.00
4	8.31	4	8.00	308	1.00
5	8.63	5	8.00	295	0.92
6	8.85	6	8.00	295	0.93
7	19.38	7	9.70	346	1.00
8	7.64	8	9.53	341	1.00
9	7.64	9	9.46	324	1.00
10	-4.23	10	9.44	328	1.00
11	-12.54	11	9.63	341	1.00
12	-12.54	12	9.36	313	1.00
13	11.87	13	9.35	306	0.98
14	3.51	14	9.25	305	0.93
15	9.12	15	9.25	305	0.95
16	0.48	16	9.33	308	1.00
17	-8.36				
18	-8.36				

Table 3 Results for estimating the effect from degradation of heat insulation

Node number	Pressure (MPa)		Temperature (°C)		Quality (-)	
6	8.00	8.00	295	295	0.67	0.93
12	9.38	9.36	312	313	1.00	1.00
13	9.37	9.35	306	306	0.98	0.98
14	9.28	9.25	306	305	0.93	0.93
15	9.28	9.25	306	305	0.67	0.95
16	9.35	9.33	306	308	0.93	1.00

Table 4 Results for connecting the mobile steam source

Node number	Pressure (MPa)	Temperature (°C)	Quality (-)
6	8.00	295	0.74
15	9.48	307	0.74

by the mobile steam source were 9.5 MPa and 307 °C. The results of nodes 6 and 15 for this condition are shown in Table 4. Owing to the saturated steam supplied by the mobile steam source, the quality at nodes 6 and 15 increased. By using the developed simulator, it is possible to evaluate and modify an existing steam distribution network and to design a new one.

Conclusions

A steam distribution network simulator for EOR systems was developed. The simulator provides: (1) highly accurate prediction of steam properties including phase change (steam to drain) in a complex steam distribution network by adopting the pipe flow model using the finite volume

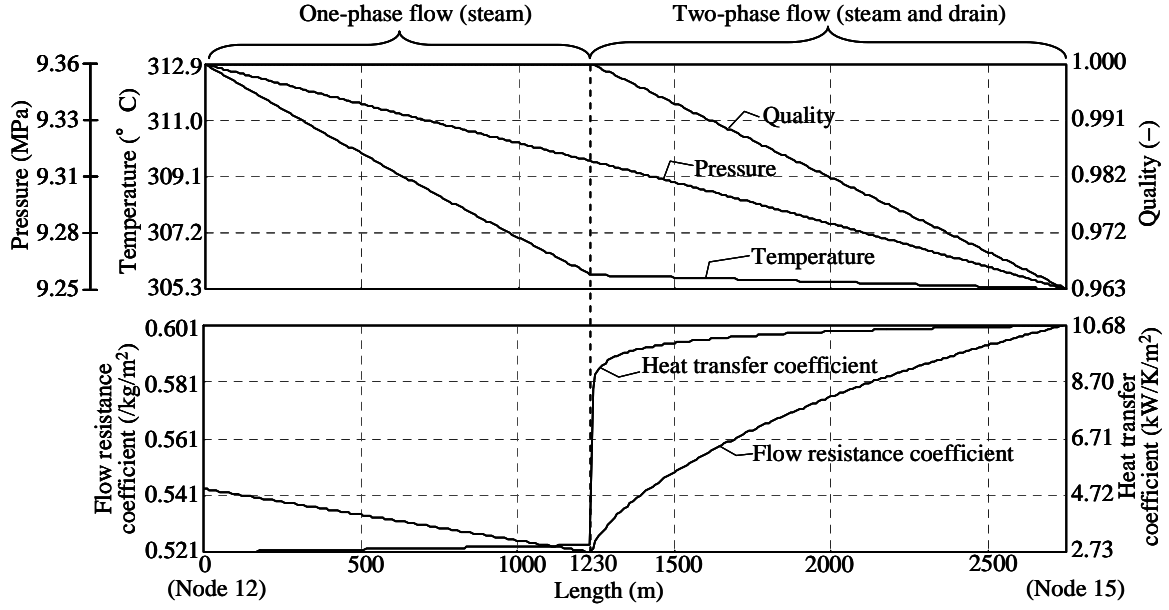


Figure 5 Steam properties along lines 17 and 18 flow

method and the Newton-Raphson method and the steam distribution network flow model according to graph theory and (2) a dedicated interface for operators to build the steam distribution network easily by referring to a topographic map. The simulation results showed that the developed simulator is useful to evaluate and modify an existing steam distribution network and to design a new one. The developed simulator is also applicable to the steam distribution network in petrochemical complexes or district heating facilities.

Acknowledgment

A part of this work was supported by the subsidies program of the Ministry of Economy, Trade and Industry, Japan.

Appendix A. Equations for wall friction force and wall heat flux

Wall friction force

The wall friction force is modeled as the product of the flow resistance coefficient K and the square of the mass flow rate which is given by

$$F_w = K(\dot{m} + \dot{m}_\varepsilon)^2 \quad (\text{A-1})$$

where \dot{m}_ε is the small mass flow rate for stabilization of pipe flow calculation. For the one-phase flow, K is expressed with the Darcy-Weisbach equation and the Swamee-Jain equation (Swamee and Jain, 1976). For the two-phase flow, K is expressed with the Nozu equation (Nozu et al., 1998).

Wall heat flux

The wall heat flux is given by the following equation

$$q_w = (T - T_{am}) / (\pi \cdot d \cdot L \cdot R) \quad (\text{A-2})$$

where

$$R = \frac{1}{2\pi \cdot L} \left(\frac{1}{r1 \cdot hi} + \frac{1}{k_m} \ln \frac{r2}{r1} + \frac{1}{k_{ins}} \ln \frac{r3}{r2} + \frac{1}{r3 \cdot ho} \right) \quad (\text{A-3})$$

The equation for the heat transfer coefficient between steam and pipe hi is switched depending on the phase status of the pipe flow. hi for the one-phase flow is expressed with the Gnielinski equation (Gnielinski, 1976) and hi for the two-phase flow is expressed with the Shah equation (Shah, 1979).

References for Appendix A

- Gnielinski, V. (1976), New equations for heat and mass transfer in turbulent pipe and channel flow, *Int. Chemical Engineering*, 16-2, pp. 359–368.
- Nozu, S., Katayama, H., Nakata, H. and Honda, H. (1998), Condensation of a refrigerant CFC11 in horizontal microfin tubes (Proposal of a correlation equation for frictional pressure gradient), *Experimental Thermal and Fluid Science*, 18, pp. 82-96.
- Shah, M. M. (1979), A general correlation for heat transfer during film condensation inside pipes, *Int. J. Heat Mass Transfer*, 22-4, pp. 547-556.
- Swamee, P. K. and Jain, A. K. (1976), Explicit equations for pipe-flow problems, *J. Hydraulics Division (ASCE: American Society of Civil Engineers)*, 102-5, pp. 657-664.

Appendix B. Nomenclature

A	Cross-sectional area (m^2)	$r3$	Pipe outer radius with heat insulator (m)
B	Incidence matrix (-)	T	Temperature ($^{\circ}C$)
b	Incidence matrix element (-)	v	Relative volume (m^3/kg)
d	Pipe inner diameter (m)	x	Vapor quality (-)
dp	Correction of pressure (Pa)	z	Space coordinate (m)
F_w	Wall friction force (N/m^3)	Δz	Control volume gird size (m)
h	Specific enthalpy (J/kg)		
hi	Heat transfer coefficient between steam and metal of pipe ($W/K/m^2$)	Greek	
ho	Heat transfer coefficient between thermal insulator and atmosphere ($W/K/m^2$)	α	Void fraction (-)
K	Flow resistance coefficient ($1/kg/m$)	Subscripts	
k	Thermal conductivity ($W/m/K$)	atm	Atmosphere
L	Pipe length (m)	G	Saturated steam
\dot{m}	Mass flow rate (kg/s)	i	Control volume gird index
\dot{m}_e	Small mass flow rate for stabilization (kg/s)	ins	Thermal insulation
m	Number of staggered grids (-)	j	Line index
N_l	Number of lines (-)	k	Node index
N_n	Number of nodes (-)	L	Saturated water
P	Wetted perimeter (m^2)	m	Metal of pipe
p	Pressure (Pa)	$line$	Value at line
q_w	Wall heat flux (W/m^2)	$node$	Value at node
R	Thermal resistance (K/W)	Superscripts	
$r1$	Pipe inner radius (m)	n	New iteration step
$r2$	Pipe outer radius without heat insulator (m)	$n-1$	Previous iteration step

References

- IAPWS (The International Association for the Properties of Water and Steam) (1997), Release on the IAPWS industrial formulation 1997 for the thermodynamic properties of water and steam, *IAPWS*, pp. 48.
- JSME (The Japan Society of Mechanical Engineers) (2006), Handbook of gas-liquid two-phase flow technology - second edition. *Corona Publishing*, pp. 70–71.
- Majumdar, A. K., Bailey, J. W. and Sarkar, B. (1997), A generalized fluid system simulation program to model flow distribution in fluid networks, *33rd AIAA/ASME/SAE/ASEE Joint Propulsion Conference*, AIAA 97-3225.
- Patankar, S. V. (1980), Numerical heat transfer and fluid flow, *Hemisphere*, pp. 118-126.
- Shamir, U., and Howard, C. D. (1968), Water distribution system analysis, *J. Hydraulics Div., Proc. Amer. Soc. Civil Engineers*, 94, pp. 219-234.
- Thom, J. R. S. (1964), Prediction of pressure drop during forced circulation boiling of water. *Int. J. Heat Mass Transfer*, 7-7, pp. 709–724.